RSC Advances

PAPER

View Article Online
View Journal | View Issue

Cite this: *RSC Adv.*, 2017, **7**, 34548

Green synthesized silver nanoparticles from *Garcinia imberti* bourd and their impact on root canal pathogens and HepG2 cell lines

S. R. Sri Ramkumar,[a] N. Sivakumar,*[b] G. Selvakumar,[c] T. Selvankumar,*[d] C. Sudhakar,[d] B. Ashokkumar[e] and S. Karthi[e]

Nanoparticle biosynthesis using the extract of medicinal plants in a non-hazardous mode has gained wide attention for various applications in nanomedicine. This study aimed to synthesize silver nanoparticles (AgNPs) using the aqueous extract of the *Garcinia imberti* and to evaluate their antibacterial and cytotoxic activities. Structural characterization of synthesized AgNPs was carried out using UV-Vis spectrophotometry, scanning electron microscopy (SEM), X-ray diffraction (XRD) and Fourier transform infrared spectroscopy (FT-IR). SEM showed the formation of particles with average sizes of 25 to 40 nm. Energy dispersive spectroscopy (EDS) was used to analyze the AgNPs within the energy range of 3–3.1 keV to detect the presence of silver. Also, the presence of the face centered solid cubic crystal structure of metallic silver was confirmed with X-ray diffraction (XRD). The functional groups of the biomolecules present in the aqueous extract of *G. imberti* and their interaction with AgNPs were identified through FT-IR analysis. The biosynthesized AgNPs exhibited antibacterial activity against root canal isolates of *Staphylococcus sciuri* S5, *Enterococcus faecalis* S9 and *Enterococcus faecium* S11. The green synthesized AgNPs showed no significant effects on HepG2 cell lines at 75 μg mL^{-1}. Thus, the biosynthesized AgNPs are found to have potential for nano-based drug delivery in future root canal treatment applications.

Received 24th December 2016
Accepted 29th June 2017

DOI: 10.1039/c6ra28328d

rsc.li/rsc-advances

1. Introduction

The synthesis of nanoparticles and their therapeutic efficacy against infectious and non-infectious disease has, impressively, attracted the attention of scientists and been investigated extensively for the last two decades worldwide.[1–3] Synthesis of noble nanoscale materials is a multidisciplinary approach converging the fields of physics, medicine, biotechnology and chemistry.[4,5] Metal based nanoparticles are very attractive, in particular because of their promising applications in various sectors and cost effectiveness.[6,7] Among them, the biosynthesis of silver nanoparticles (AgNPs) seems to be advantageous for biomedical applications, especially in therapeutic interventions because of their characteristic physiological and biological properties.[8–10] AgNPs are known to have promising biological potential including antimicrobial,[11] antioxidant,[12] anti-cancer,[13,14] antidiabetic,[15] antifungal,[16,17] anti-inflammatory,[18] antiviral,[19] antiangiogensis[20] and antiplatelet[21] activities.

Silver nanoparticles emanated as potent antimicrobial compounds with enhanced efficacy against Gram-positive and Gram-negative bacteria, including drug resistant strains, and are the best suited alternatives for antibiotics that pose a menace for bacterial resistance to drugs. Generally, silver in its ionic[22,23] or metallic form has high antimicrobial activity through rapidly binding to a variety of negatively charged molecules (proteins, DNA and RNA) in the pathogens.[24] The search for eco-friendly, more promising and cost effective strategies to synthesize nanoparticles offered a better way of exploring vast biodiversity especially plants sources for greener biosynthesis of nanoparticles. The green synthesis of nanoparticles using herbal extracts has superior biological activities and proven as less toxic to human.[25] Plant extract based synthesis of AgNPs and its bio-potentials are well documented with *Ficussy comorus*,[26] *Myristica fragrans*,[27] *Helianthus tuberosus*,[28] *Tinospora cordifolia*,[29] *Chrysanthemum indicum* L.,[30] *Mimusops elengi* L.,[31] and *Azadirachta indica* L.[32] *Garcinia imberti* bourd is an endangered plant belongs to the family Clusiaceae found evergreen in the South Western Ghats, India, which has better antioxidant[33] as well as antimicrobial activity.[34] However,

[a]*Department of Microbiology, Bharathiar University, Coimbatore, Tamil Nadu, India*
[b]*Department of Molecular Microbiology, School of Biotechnology, Madurai Kamaraj University, Madurai 625 021, Tamil Nadu, India. E-mail: microshivaak@gmail.com; Tel: +91-9445389174*
[c]*Department of Microbiology, Alagappa University, Karaikudi 630003, Tamil Nadu, India*
[d]*PG & Research Department of Biotechnology, Mahendra Arts and Science College (Autonomous), Kalippatti, Namakkal 637 501, Tamil Nadu, India. E-mail: t_selvankumar@yahoo.com; Tel: +91-9443470394*
[e]*Department of Genetic Engineering, School of Biotechnology, Madurai Kamaraj University, Madurai 625 021, Tamil Nadu, India*

no attempts have been made so far to use *Garcinia imberti* bourd extract for green biosynthesis of AgNPs. Hence, in this study, the aqueous extract of *Garcinia imberti* bourd leaf was used to synthesize AgNps for the first time and also investigated their antibacterial potentials against root canal pathogens such as *Staphylococcus sciuri* S5, *Enterococcus faecalis* S9 and *Enterococcus faecium* S11 and cytotoxic activity on HepG2 cell lines.

2. Materials and method

2.1. Preparation of *G. imberti* bourd leaf extract

The *G. imberti* bourd, leaves were collected from evergreen forest of Western Ghats, Kerala, India. The dust and other adherent materials were completely removed by washing with tap water and then rinsed with double distilled water. Then it was shadow dried and pulverized to get a uniform size (0.3 mm). Fifty grams of dried leaf powder was taken in cellulose cartridge Whatman no. 1 paper (30 mm × 100 mm) and subjected to soxhlet extraction with 200 mL of solvents (water). This experimental setup was run for 8 h at 80 °C. The solvent was allowed to be evaporated by keeping it in water bath (60 °C) until a constant weight was obtained. Eventually the resulting extracts were weighed and collected in a sterile McCartney bottles and then stored in refrigerator (4 °C) for further study.

2.2. Biosynthesis of AgNPs

For the synthesis of AgNPs, 50 mL of aqueous silver nitrate ($AgNO_3$) at a concentration of 1 mM was added with 5 mL of leaf extract at dark, mixed properly, and incubated at room temperature for 48 h.[11] The aqueous leaf extract reduced and stabilized the $AgNO_3$ into AgNPs, which can be seen visually by the change of colourless mixture to dark brown.

2.3. Characterization of biosynthesized AgNPs

The bio-reduction of Ag^+ ions in solutions was evaluated by a UV-Vis spectrophotometer (Elico SL-164 PC), at a range between 300 and 700 nm with 1 nm resolution. Aqueous silver nitrate (1 mM) was used as a blank.[35] The AgNPs shape and size was determined by scanning electron microscopy-energy-dispersive spectra (SEM-EDS-JEOL JSM 6390 model). X-ray diffraction data (XRD) was recorded in the 2θ range of 30–80° using XRD6000, (Shimadzu) of Cu-Kα radiation, the energy of which was 8.04 keV and wavelength was 1.54 Å. The applied voltage was 40 kV and current was 25 mA. The crystallite size was estimated using the Scherer equation.[36] FT-IR analysis was performed with a mixture containing powdered potassium bromide (KBr) and lyophilized leaf extract. To record the molecular functional vibration of chemical groups present in the sample, Perkin-Elmer FT-IR spectrum-1 spectrophotometer (Shimadzu 8400) was used and operated at a resolution of 2 cm^{-1} ranging from 4000 to 400 cm^{-1}.

2.4. Antibacterial activity of AgNPs

Agar well diffusion method[37] was used to test antibacterial activity of AgNps against *Staphylococcus sciuri* S5, *Enterococcus faecalis* S9 and *E. faecium* S11 (isolates of root canal samples), for this, Muller–Hinton (MH) agar plates were initially seeded with overnight cultures (0.1 O.D.) of those test organisms. Using sterile well punctures (6 mm dia.), wells were made on medium and 30 μL of AgNps (dissolved in sterile buffered phosphate saline) at a concentration of 5 μg per well and 10 μg per well were added. After incubation of plates at 37 °C for 24 h, zone of inhibition around the wells was measured. Experiments were performed in triplicate and calculated the mean value. Ampicillin (100 μg per well) was used as the positive control.

2.5. Determination of minimum inhibitory concentration (MIC) and minimum bactericidal concentration (MBC)

The MIC was determined in nutrient broth dilution method using aqueous extract of *G. imberti* and AgNPs as test samples. Briefly, 3 mL of sterile nutrient broth adjusted with 1000 μg mL^{-1} of the test samples and two fold serial dilutions was made in similar volume of broth up to 3.9 μg mL^{-1} and 100 μL of overnight test culture (0.1 O.D. value; 600 nm) was added to the tubes. Both positive (with bacterial inoculum) and negative control (without bacterial inoculum) were maintained. After 16 h of bacterial growth at 37 °C, turbidity of the culture tubes were determined by spectrophotometrically at 595 nm. The lowest dilution which completely inhibits the visible bacterial growth was considered as MIC. Aliquots of 100 μL culture from all dilutions were seeded in nutrient agar plates and incubated for 24 h at 37 °C. The MBC was determined by the presence or absence of bacterial growth in agar plates after incubation.

2.6. Determination of bacterial growth curves after AgNPs treatment

To determine the bacterial growth curve, cells were exposed to AgNPs at the concentrations of 0, IC_{50} and MIC. For this, 50 mL of nutrient broth in 100 mL conical flask were adjusted with the AgNP at IC_{50} (200 μg mL^{-1} for *S. sciuri* S5, 270 μg mL^{-1} for *E. faecalis* S9 and 180 μg mL^{-1} for *E. faecium* S11), MIC (250 μg mL^{-1} for *S. sciuri* S5, 250 μg mL^{-1} for *E. faecalis* S9 and 125 μg mL^{-1} for *E. faecium* S11) and without AgNP, which was used as control (positive). Bacterial inoculums (1%) were given at the concentration of 0.1 O.D. at 600 nm. Culture setup was kept in shaking condition (120 rpm), for 24 h at 37 °C and every 3 h interval an aliquot of bacterial suspension was aseptically transferred to measure the bacterial growth in terms of turbidity at 600 nm (Elico SL-164, double beam UV-Vis spectrophotometer) against uninoculated control (blank).

2.7. *In vitro* cell viability assay

The cytotoxicity of AgNPs on HepG2 cells (ATCC HB 8065) procured from NCCS, Pune, India and the cells were used to determine the MTT assay (3-(4,5-dimethyl thiazol-2yl)-2,5-diphenyl tetrazolium bromide).[38] For this, HepG2 cells were cultured in DMEM medium supplemented with inactivated fetal calf serum (10%) at 37 °C in an incubator at humidified atmosphere with 5% CO_2. In order to find the cytotoxicity, the cells were seeded at a density of 1×10^4 per well in a 96-well microtiter plate. Grown cells were replaced with fresh medium containing varying concentrations of nanoparticles (0, 25, 50

and 75 μg mL^{-1}) after the removal of spent medium. Following 24 h of incubation, 20 μL of MTT dye solution (5 mg mL^{-1} in phosphate buffer pH 7.4, MTT Sigma) was added to each well and incubated for 6 h at 37 °C in a CO_2 incubator to assess cell cytotoxicity. DMSO (0.1 mL) was further added to each well, mixed properly and left for 15 min. Development of purple color due to the formation of formazan crystals indicates the presence of viable cells. The absorbance of each well was read on a microplate reader at 595 nm and the effect of nanoparticles on relative cell viability (%) was calculated by comparing with the control using this equation.

$$\text{The relative cell viability (\%)} = \text{test OD/control OD} \times 100$$

3. Results and discussion

3.1. Biosynthesis of AgNPs

This study describes the green biosynthesis of AgNPs using the aqueous extract of *G. imberti* leaves, which begins with addition of 1 mM $AgNO_3$ at room temperature. Changing of colour from light green to dark brown (Fig. 1(a)) is due to the vibrations of excitation of surface plasmon resonance (SPR) in AgNPs, indicating the transition of silver ion (Ag^+) to silver nanoparticle (Ag^0)[39] and confirmed the biosynthesis of AgNPs. Similar results were observed earlier with *Acorus calamus* rhizome extract.[11]

3.2. Characterization of AgNPs

The synthesized AgNPs was assessed by measuring absorption spectrum using UV-Vis spectrophotometer, a strong absorption peak was obtained at 420 nm (Fig. 1(b)). The high-quality absorption peak implied that the preparation has narrow sized nanoparticles. The surface plasmon response banding at 420 nm indicates the synthesis of AgNPs.[40] Similar result was reported by Lokina *et al.*,[41] while Bhimba *et al.*[42] showed the absorption spectrum of AgNPs with maximum at 424 nm, which may be due to the variance in particle size. The Fourier transform infrared spectroscopy (FT-IR) used to identify the potential reducing agent responsible as synthesized AgNPs (Fig. 2). The peak at positions 3414 cm^{-1} and 2920 cm^{-1} was due to the stretching of the O–H band of amino groups or H groups indicating the presence of alcohols, phenols. The peaks at 2854 cm^{-1} and 1374 cm^{-1} indicates the C–H stretch; 1709 cm^{-1} specify the C=O bond, 1621 cm^{-1} shows N–H bend and 1044 cm^{-1} indicates C–N positions of the biomolecule. The peak that appeared around 2928 cm^{-1} related to the stretching of the C–H bonds.[33] The peak at 1709 cm^{-1} was due to C=O stretch of carbonyls in proteins 10. Peaks obtained from FT-IR spectrum of AgNPs, showed number of bands between 1044 cm^{-1} to 828 cm^{-1} due to C–O, C–N stretching vibrations of alcohols, ethers, esters and amines.[43,44] Presence of the functional groups implied that the extract has bioreductant molecules, which might be responsible for synthesis of AgNPs. Similar results were observed earlier when *Erythrina indica* root extract was used for the synthesis of silver nanoparticles.[13]

The XRD pattern of AgNPs is shown in Fig. 3, where four characteristic peaks were detected in at 2 h analysis with the values of 38.68°, 44.1°, 64.11° and 77.4° corresponding to 111,

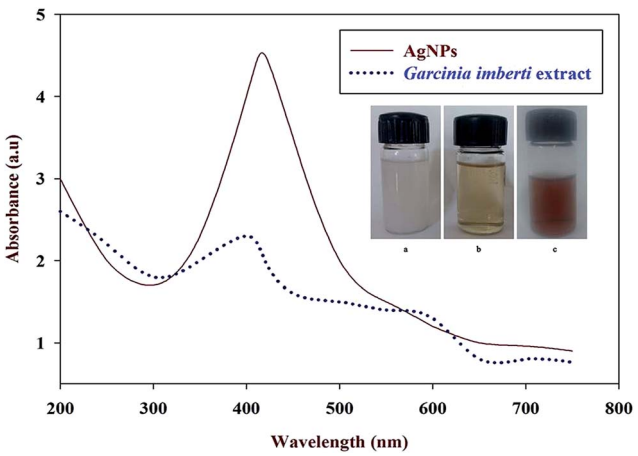

Fig. 1 UV-Vis absorption spectra of biosynthesized AgNPs and the aqueous extract of *G. imberti* bourd. (a) 1.0 mM $AgNO_3$ solution, (b) aqueous extract of *G. imberti* bourd, and (c) synthesized AgNPs.

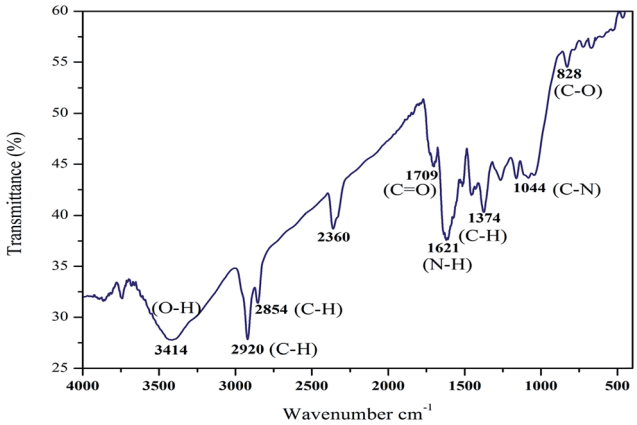

Fig. 2 FT-IR spectrums of AgNPs synthesized by aqueous extract of *G. imberti*.

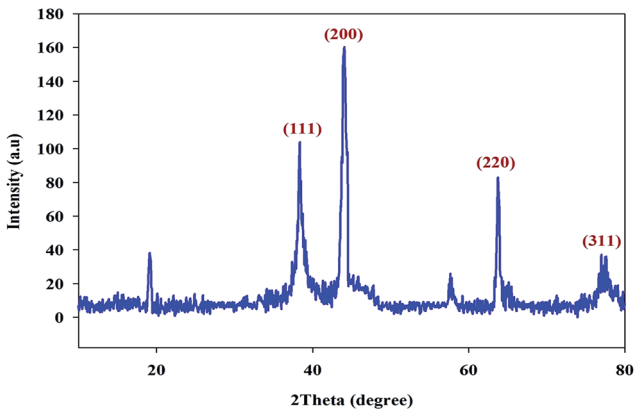

Fig. 3 XRD pattern of biosynthesized AgNPs.

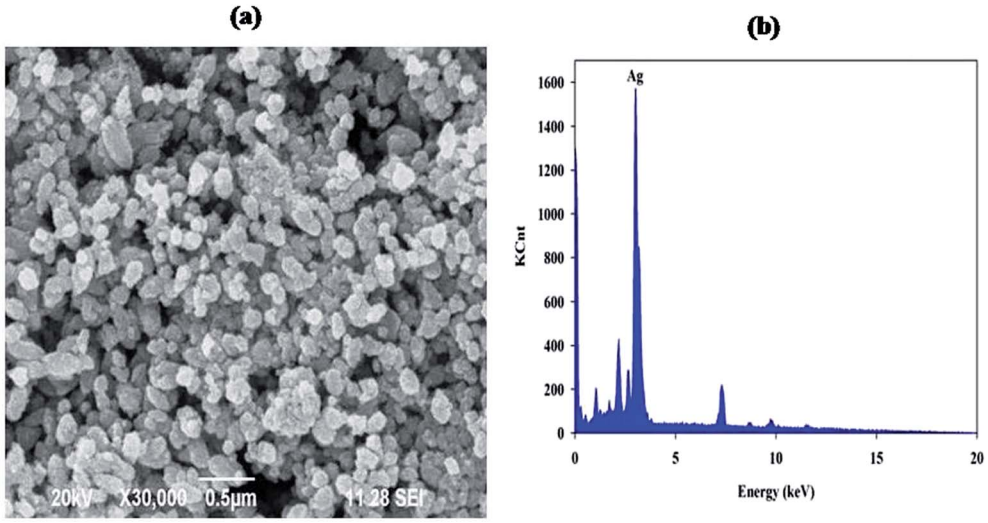

Fig. 4 (a) SEM images of AgNPs shows spherical shape (b) conformation of elemental silver in AgNPs by EDS spectrum.

200, 220 and 311 crystalline planes of face centered cubic (fcc) solid crystalline structure of metallic silver. These observations were corroborated to some extent with the findings reported previously[44] and were also compatible with the database of the Joint Committee on Powder Diffraction Standards (JCPDS) file no. 04-0783. The detection of no other peaks from any other phase evidenced that single-phase Ag with cubic structure nanoparticles has been obtained directly. Based the on Debye–Scherrer equation, the average crystallite size of AgNPs was found to as 17 nm, which was comparatively similar as reported earlier by Kalpana *et al.*[45] Through SEM analysis, size of the AgNPs synthesized by *G. imberti* extract was found to be cubic in shape with the average size of 27 nm (Fig. 4(a)). The EDX results of AgNPs showed strong signals for silver particles (Fig. 4(b)), which confirmed the presence of AgNPs based on its strong energy peaks around 3–3.1 keV.[20]

3.3. Anti-bacterial activity of synthesized AgNPs

The antibacterial activity of the synthesized AgNPs against root canal pathogens is shown in the Fig. 5. The bactericidal activity

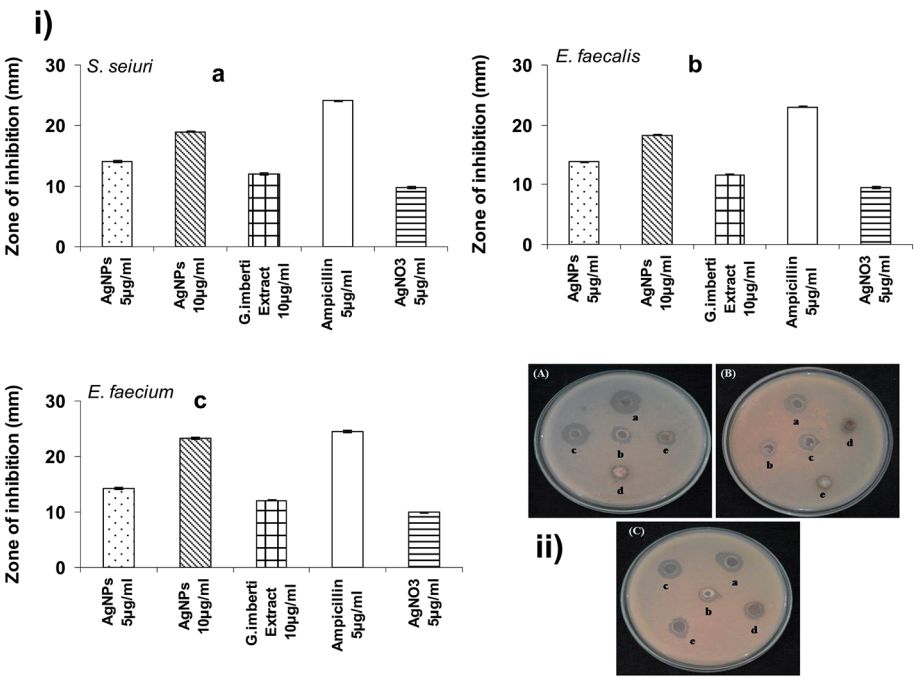

Fig. 5 (i) Antibacterial activity of *G. imberti* leaf aqueous extract and extract mediated synthesized AgNPs. (ii) Mueller–Hinton agar plates showing zone inhibition by (a) ampicillin (5 μg mL^{-1}), (b) AgNPs (5 μg mL^{-1}), (c) AgNPs (10 μg mL^{-1}), (d) plant extract (10 μg mL^{-1}) and (e) $AgNO_3$ (5 μg mL^{-1}); *Staphylococcus sciuri* S5 (A), *Enterococcus faecalis* S9 (B) and *Enterococcus faecium* S11 (C).

Table 1 MIC and MBC values of silver nanoparticles

	G. imberti extract (μg mL^{-1})		$AgNO_3$ (μg mL^{-1})	
Organism	MIC	MBC	MIC	MBC
S. seiuri	250	500.0	62.5	250
E. faecalis	250	500.0	62.5	250
E. faecium	125	250.0	31.25	125

of AgNPs was found to be high against *E. faecium* (14.4 mm) and comparatively less with *E. faecalis* (10.4 mm), and *S. sciuri* (11 mm). The activity showed by the aqueous plant extract was lesser than the synthesized AgNPs, whereas increased activity may be due to the presence of reduced silver ions. Silver ions readily bind on the cell membrane and affect the respiratory functions of the cell,[46–48] hence the AgNPs has pronounced antibacterial activity. Biosynthesized AgNPs with smaller size showed maximum antibacterial activity than the AgNPs in larger size, which might be due to the interaction as well as penetration of particle in to the bacterial cell,[49,50] also it results in diminished chances of developing bacterial resistance.[51] Previously, it has been well demonstrated that oxidized form of silver ion has broad spectrum of antimicrobial activity against Gram-positive and Gram-negative bacteria,[52] because silver ions are capable of binding efficiently with electron donor groups like sulphur and oxygen present in bacterial cell wall leading cellular content leakage by cell wall damage and ultimately results in cell death.[53,54]

3.4. MIC and MBC of AgNPs

Following exposure of bacteria at different concentrations of AgNPs for 24 h, its growth was monitored and the MIC and MBC of *E. faecalis* was observed maximum at a concentration of 62.5 μg mL^{-1} and 250 μg mL^{-1}, which indicated that AgNPs has both the bacteriostatic and bactericidal activities (Table 1). While, aqueous extract of $AgNO_3$ showed the MIC and MBC of 250 μg mL^{-1} and 500 μg mL^{-1} only. Low MIC (31.25 μg mL^{-1}) and MBC (125 μg mL^{-1}) of AgNPs was observed against *E. faecium*, which confirmed that *E. faecium* was the most susceptible organism for AgNPs. Krishnan *et al.*[55] has previously reported that 5 mg mL^{-1} as the optimum MIC concentration of AgNPs against *E. faecalis*. Generally, it is known that the particle size of the AgNPs causes variation on bacterial inhibition as well as bacterial lysis. The nanoparticles with ultrafine size cause its action at very low concentrations. In this study, synthesized AgNPs have the size of 27 nm, which has high bactericidal and bacteriostatic activity even at 62.5 μg mL^{-1} concentration. However, for AgNPs with less than 10 nm size, the antibacterial efficacy was significantly high due to delayed bacterial growth kinetics.[56]

3.5. Growth curves of bacterial cells treated with AgNPs

Bacterial growth curve were determined in the presence of AgNPs by measuring O.D. at different time point to indicate the inhibitory action of nanoparticles on its multiplication. The growth curves of AgNPs treated *S. sciuri*, *E. faecalis* and *E. faecium* cells are shown in Fig. 6. The bacterial growth in IC_{50}

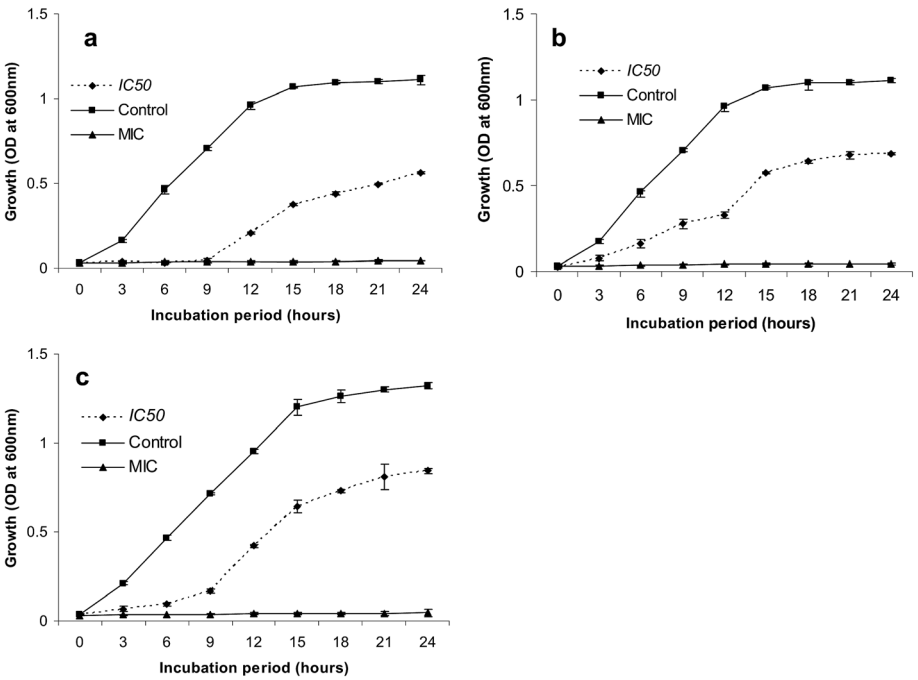

Fig. 6 Effect of MIC and IC_{50} concentration of AgNPs on bacterial growth. 10^5 cfu per mL of bacterial inoculum was given in media with MIC and IC_{50} concentrations of AgNPs and incubated for 24 h at 37 °C. *Staphylococcus sciuri* S5 (a), *Enterococcus faecalis* S9 (b) and *Enterococcus faecium* S11 (c). The assay was performed in triplicate; the error bars indicate the SD.

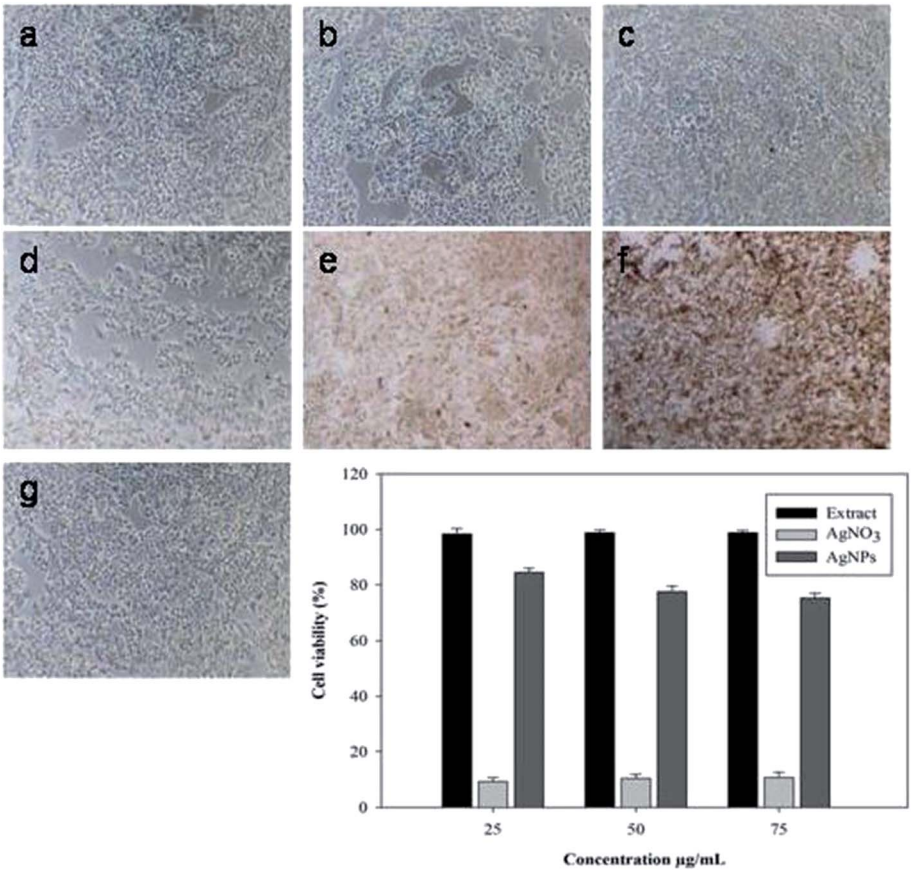

Fig. 7 Effects of AgNPs on HepG2 cell viability. *G imberti* aqueous extract at 25 μg mL^{-1} (a) and 75 μg mL^{-1} (b); AgNPs 25 μg mL^{-1} (c) and 75 μg mL^{-1} (d); $AgNO_3$ at 25 μg mL^{-1} (e) and 75 μg mL^{-1} (f); DMSO control group (g).

concentration of AgNPs treated cells were significantly inhibited around ~50%. Bacterial growth inhibition was observed up to 9 h of incubation after that growth was increased due to lowering concentration of AgNPs, which was not adequate enough to inhibit bacterial growth, and thus the bacterium starts multiply and grows well. These findings clearly indicated that the AgNPs mediate antibacterial activity by affecting its reproduction and inhibits the growth of actively dividing bacterial cells.

3.6. Cell viability assay

The results of MTT assays showed a dose-dependent loss of viability of HepG2 cell line after 24 h exposure to aqueous plant extract, $AgNO_3$ and AgNPs (Fig. 7). Results of HepG2 cell viability assay revealed the lowest concentration of $AgNO_3$ rapidly decreases the viability, but the nano preparations exerted no effects on the viability of cells. HepG2 cells were not affected even with high concentration of extract and AgNPs (75 μg mL^{-1}), but even at low concentration of biosynthesized AgNPs (25 μg mL^{-1}) completely killed the bacterial cells, which indicated that plant extract and AgNPs doesn't cause any cytotoxic activity on HepG2 cells. Generally, bacteria have a larger surface area-to-volume ratio than eukaryotic cells, which allows for rapid uptake and intracellular distribution of NPs.[57]

4. Conclusion

This study presents green synthesis of non-toxic and economically viable AgNPs by using aqueous extract of an endangered plant *Garcinia imberti* for the first time. The biosynthesized AgNPs are spherical and single crystalline in shape with a size of 27 nm. The antibacterial activity of AgNPs revealed potential inhibitory activity against *E. faecium*, *S. sciuri*, and *E. faecalis*. Hence, the plant mediated biosynthesis of AgNPs can be used as good therapeutic agent against human pathogens and also for the successful development of nanomedicine in future.

Acknowledgements

Authors are acknowledged to DST-PURSE, M. K. University, Madurai for providing the instrumentation support.

References

1 P. Raveendran, J. Fu and S. L. Wallen, *J. Am. Chem. Soc.*, 2003, **125**, 13940.
2 R. Bhattacharya and P. Mukherjee, *Adv. Drug Delivery Rev.*, 2008, **60**, 1289.
3 Y. Park, Y. N. Hong, A. Weyers, Y. S. Kim and R. J. Linhardt, *IET Nanobiotechnol.*, 2011, **5**, 69.

4 C. Dipankar and S. Murugan, *Colloids Surf., B*, 2012, **98**, 112.
5 P. Prakash, P. Gnanaprakasam, R. Emmanuel, S. Arokiyaraj and M. Saravanan, *Colloids Surf., B*, 2013, **108**, 255.
6 H. Huang and Y. Yang, *Compos. Sci. Technol.*, 2008, **68**, 2948.
7 C. G. Yuan, C. Huo, B. Gui, P. Liu and C. Zhang, *J. Cluster Sci.*, 2016, **28**, 1319.
8 R. Jin, Y. C. Cao, E. Hao, G. S. Métraux, G. C. Schatz and C. A. Mirkin, *Nature*, 2003, **425**, 487.
9 A. Tricoli and S. E. Pratsinis, *Nat. Nanotechnol.*, 2010, **5**, 54.
10 Y. Kuthati, R. K. Kankala, S. X. Lin, C. F. Weng and C. H. Lee, *Mol. Pharmaceutics*, 2015, **112**, 2289.
11 C. Sudhakar, K. Selvam, M. Govarthanan, B. Senthilkumar, A. Sengottaiyan, M. Stalin and T. Selvankumar, *J. Genet. Eng. Biotechnol.*, 2015, **13**, 93.
12 V. Vilas, D. Philip and J. Mathew, *Mater. Sci. Eng.*, 2016, **61**, 429.
13 A. Sengottaiyan, C. Sudhakar, K. Selvam, T. Selvankumar, M. Govarthanan, B. Senthikumar and K. Manoharan, *Int. J. Tra. Complementary Med.*, 2016, **1**, 0001.
14 O. Muhammad, T. K. Ali, R. Abida, A. K. Muhammad, A. Irshad, U. I. Nazar, S. Muthupandian, F. U. Muhammad, A. Muhammad and K. S. Zabta, *Nanomedicine*, 2006, **11**, 3157.
15 A. Sengottaiyan, A. Aravinthan, C. Sudhakar, K. Selvam, P. Srinivasan, M. Govarthanan, K. Manoharan and T. Selvankumar, *JNSC*, 2016, **6**, 41.
16 G. Chladek, A. Mertas, I. Barszczewska-Rybarek, T. Nalewajek, J. Zmudzki, W. Krol and J. Lukaszczyk, *Int. J. Mol. Sci.*, 2011, **7**, 4735.
17 H. Barabadi, S. Honary, M. Ali Mohammadi, E. Ahmadpour, M. Taghi Rahimi, A. Alizadeh, F. Naghibi and M. Saravanan, *Environ. Sci. Pollut. Res.*, 2017, **24**, 5800.
18 F. Martinez-Gutierrez, E. P. Thi and J. M. Silverman, *Nanomedicine*, 2012, **3**, 328.
19 A. Mohammed Fayaz, Z. Ao, M. Girilal, L. Chen, X. Xiao, P. Kalaichelvan and X. Yao, *Int. J. Nanomed.*, 2012, **7**, 5007.
20 K. Kang, D. H. Lim, I. H. Choi, T. Kang, K. Lee, E. Y. Moon, Y. Yang, M. S. Lee and J. S. Lim, *Toxicol. Lett.*, 2011, **3**, 227.
21 V. M. Ragaseema, S. Unnikrishnan, V. Kalliyana Krishnan and L. K. Krishnan, *Biomaterials*, 2012, **11**, 3083.
22 A. B. Smetana, K. J. Klabunde and C. M. Sorensen, *J. Colloid Interface Sci.*, 2005, **284**, 521.
23 R. Emmanuel, S. Palanisamy, C. Shen-Ming, K. Chelladurai, S. Padmavathy, M. Saravanan, M. Ajmal Ali and M. A. H. Fahad, *Mater. Sci. Eng., C*, 2015, **56**, 374.
24 T. J. Berger, J. A. Spadaro, S. E. Chapin and R. O. Becker, *Antimicrob. Agents Chemother.*, 1976, **9**, 357.
25 S. Lokina, A. Stephen, V. Kaviyarasan, C. Arulvasu and V. Narayanan, *Eur. J. Med. Chem.*, 2014, **9**, 256.
26 W. M. Salema, M. Haridy, W. F. Sayed and N. H. Hassan, *Ind. Crops Prod.*, 2014, **62**, 228.
27 B. Senthilkumar, S. Ilakkia, K. Selvam, D. Senbagam, S. K. Nachimuthu and G. Guruswami, *Environ. Sci. Pollut. Res.*, 2017, **14**, 14758.
28 A. Aravinthan, M. Govarthanan, K. Selvam, L. Praburaman, T. Selvankumar, R. Balamurugan, S. Kamala-Kannan and J.-H. Kim, *Int. J. Nanomed.*, 2015, **10**, 1977.
29 K. Selvam, C. Sudhakar, M. Govarthanan, P. Thiyagarajan, A. Sengottaiyan, B. Senthilkumar and T. Selvankumar, *J. Radiat. Res. Appl. Sci.*, 2017, **10**, 6.
30 S. Arokiyaraj, V. Dinesh Kumar, V. Elakya, T. Kamala, S. K. Park, M. Ragam, M. Saravanan, M. Bououdina, M. V. Arasu, K. Kovendan and S. Vincent, *Environ. Sci. Pollut. Res.*, 2015, **22**, 9759.
31 P. Prakash, P. Gnanaprakasam, R. Emmanuel, S. Arokiyaraj and M. Saravanan, *Colloids Surf., B*, 2013, **108**, 255.
32 V. Palaniyandi, D. Jayabrata, P. Raman, V. Baskaralingam and P. Kannaiyan, *Ind. Crops Prod.*, 2015, **66**, 103.
33 K. Rajkumar, R. Shubharani and V. Sivaram, *Int. J. Pharma Sci. Res.*, 2015, **9**, 4016.
34 K. B. Ramesh Kumar, S. Shiuraj and V. George, *Journal of Tropical Medicinal Plants*, 2005, **2**, 271.
35 S. J. Ahn, S. J. Lee, J. K. Kook and B. S. Lim, *Dent. Mater.*, 2009, **25**, 206.
36 A. Monshi, M. Reza Foroughi and M. Reza Monshi, *World J. Nano Sci. Eng.*, 2012, **2**, 154.
37 A. Nanda and M. Saravanan, *Nanomedicine*, 2009, **5**, 452.
38 T. Mosmann, *J. Immunol. Methods*, 1983, **65**, 55.
39 B. Valentin Bhimba, S. S. Gurung and U. Nandhini, *Int. J. ChemTech Res.*, 2015, **7**, 68.
40 A. D. Dwidedi and K. Gopal, *Colloids Surf., A*, 2010, **369**, 27.
41 S. Lokina, A. Stephen, V. Kaviyarasan, C. Arulvasu and V. Narayanan, *Eur. J. Med. Chem.*, 2014, **76**, 256.
42 B. V. Bhimba, J. Saraniya Devi and S. Usha Nandhini, *Indian J. Biotechnol.*, 2015, **14**, 276.
43 P. Mulvaney, *Langmuir*, 1996, **12**, 788.
44 V. Vidya, P. Daizy and M. Joseph, *Spectrochim. Acta, Part A*, 2014, **132**, 743.
45 D. Kalpana, J. H. Han, W. S. Park, S. M. Lee, R. Wahab and Y. S. Lee, *Arabian J. Chem.*, 2014, DOI: 10.1016/j.arabjc.2014.08.016.
46 S. Muthukrishnan, S. Bhakya, T. Senthil Kumar and M. V. Rao, *Ind. Crops Prod.*, 2015, **63**, 119.
47 N. S. Sankar, P. Dipak, H. Nilu, S. Dipta and K. P. Samir, *Appl. Nanosci.*, 2015, **5**, 703.
48 S. Arokiyaraj, S. Vincent, M. Saravanan, Y. Lee, Y. Kyoon Oh and K. Hoon Kim, *Artif. Cells, Nanomed., Biotechnol.*, 2017, **45**, 372.
49 M. J. Catalina and E. M. V. Hoek, *J. Nanopart. Res.*, 2010, **12**, 1531.
50 J. R. Morones, J. L. Elechiguerra, A. Camacho, K. Holt, J. B. Kouri, J. T. Ramırez and M. J. Yacaman, *Nanotechnology*, 2005, **16**, 2346.
51 J. G. Holler, S. B. Christensen, H. C. Slotved, H. B. Rasmussen, A. Guzman, C. E. Olsen, B. Petersen and P. Molgaard, *J. Antimicrob. Chemother.*, 2012, **67**, 1138.
52 N. Stobie, B. Duffy, D. E. McCormack, J. Colreavy, M. Hidalgo, P. McHale and S. J. Hinder, *Biomaterials*, 2008, **29**, 963.
53 C. Damm, H. Munstedt and A. Rosch, *Mater. Chem. Phys.*, 2008, **108**, 61.

54 P. Srinivasan, S. Sudhakar, A. Sengottaiyan, P. Subramani, C. Sudhakar, K. Manoharan and P. Thiyagarajan, *Int. J. Adv. Sci. Eng.*, 2015, **1**, 42.
55 R. Krishnan, V. Arumugam and S. K. Vasaviah, *J. Nanomed. Nanotechnol.*, 2015, **6**, 1.
56 S. Agnihotri, S. Mukherji and S. Mukherji, *RSC Adv.*, 2014, **4**, 3974.
57 K. Y. Yoon, J. H. Byeon, J. H. Park, J. H. Ji, G. N. Bae and J. Hwang, *Environ. Eng. Sci.*, 2008, **25**, 289.